Inhibition of Heat Shock Protein 90 in the Spinal Cord Improves the Therapeutic Index of Morphine

David I. Duron,[1] Katherin A. Gabriel,[1] Jessica L. Bowden,[1] Christopher S. Campbell,[1] Sanket Mishra,[2] Brian S.J. Blagg,[2] and John M. Streicher[1*]

[1]Department of Pharmacology, College of Medicine, University of Arizona, Tucson AZ

[2]Department of Chemistry and Biochemistry, College of Science, University of Notre Dame, Notre Dame IN

***Corresponding Author:** John M. Streicher, Ph.D.; University of Arizona College of Medicine, Box 245050 LSN563, 1501 N. Campbell Ave., Tucson AZ 85724. Ph: (520)-626-7495

Email: jstreicher@arizona.edu

ORCID: John Streicher 0000-0002-4173-7362

Keywords: Heat shock protein 90, opioid, anti-nociception, reward, constipation, tolerance, therapeutic index

Running Title: Spinal Hsp90 Inhibition Improves Opioid Therapy

Number of Figures: 7

Number of Tables: 1

Abstract

Opioid drugs are the gold standard for treating acute and chronic pain, but are limited by negative side effects, including tolerance, constipation, and addiction. New approaches are thus greatly needed to improve opioid therapy and decrease side effects. Our investigations have revealed Heat shock protein 90 (Hsp90) as a critical regulator of opioid receptor signaling, and that inhibition of spinal cord Hsp90 boosts opioid anti-nociception. These findings led us to hypothesize that spinal Hsp90 inhibitor treatment could improve the therapeutic index of opioids, boosting anti-nociception while improving or not altering side effects, enabling a dose-reduction strategy. To test this hypothesis, we injected the Hsp90 inhibitor KU-32 by the intrathecal route into male and female CD-1 mice. We then tested these mice for their response to morphine in a battery of anti-nociception and side effect models. We found that spinal KU-32 treatment increased the anti-nociceptive potency of morphine by 2-4 fold in the tail flick, post-surgical paw incision, and HIV peripheral neuropathy pain models. At the same time, morphine anti-nociceptive tolerance was reduced from 21 fold to 2.9 fold by KU-32 treatment, and established morphine tolerance could be rescued by KU-32 injection. Reward as measured by conditioned place preference and constipation were both unchanged. These results support our hypothesis, and suggest that Hsp90 inhibitors could be a novel approach to improve the therapeutic index of opioids, enable a dose-reduction strategy, and lead to fewer side effects during pain therapy.

Abbreviations: 90 kDa Ribosomal S6 Kinase (RSK); Area Under the Curve (AUC); Conditioned Place Preference (CPP); Dimethylsulfoxide (DMSO); Extracellular Signal-Regulated Kinase Mitogen Activated Protein Kinase (ERK MAPK); Heat shock protein 90 (Hsp90); High Performance Liquid Chromatography (HPLC); High Resolution Mass Spectrometry (HRMS); Maximum Possible Effect (MPE); Nuclear Magnetic Resonance (NMR); United States Pharmacopeia (USP);

Introduction

Chronic pain is a serious health concern, affecting more than 100 million people in the United States alone with an economic cost of more than $600 billion per year [16]. Opioid drugs like morphine are often the only efficacious option for moderate to severe pain, as alternatives like tricyclic antidepressants and gabapentinoids show limited efficacy, with 50% number needed to treat values of 6 or higher in recent studies [15]. However opioids have strong limitations; they are ineffective for some pain types such as neuropathic or musculoskeletal pain [6], and they are plagued by a host of side effects, including tolerance, constipation, reward/addiction, and respiratory depression, which impact patient quality of life and have contributed to an opioid abuse and overdose crisis [3; 40]. These limitations suggest the need for new approaches to improve opioid therapy and decrease side effects, which has not been successful to date.

To this end we've engaged in an investigation into the role of Heat shock protein 90 (Hsp90) in regulating opioid receptor signaling and anti-nociception. Hsp90 is a ubiquitous and highly expressed chaperone protein with a variety of roles and client proteins; these roles range from promoting proper nascent protein folding to regulating acute kinase signal transduction (reviewed in [27; 36]). Hsp90 has mostly been studied in the context of cancer. A few papers have shown that Hsp90 promotes inflammation during inflammatory and neuropathic pain [17; 20; 26], and another two papers have shown that Hsp90 could promote opioid dependence and withdrawal [1; 21]. More recently, another paper has linked the Hsp90β isoform to opioid receptor signaling [45]. However, in general, the role of Hsp90 in the pain and opioid systems is mostly unstudied (reviewed in [35]).

In our work, we've uncovered a role for Hsp90 in opioid signaling and anti-nociception that differs between the brain and spinal cord. In brain, Hsp90 promotes ERK MAPK signaling via the Hsp90α isoform and the co-chaperones Cdc37 and p23; Hsp90 inhibitor treatment in the brain thus reduces ERK MAPK signaling and opioid anti-nociception [22; 24; 33]. In contrast, Hsp90 represses opioid anti-nociception and signaling in the spinal cord, so that Hsp90 inhibitor treatment in the spinal cord promotes an ERK-RSK signaling cascade that results in enhanced opioid anti-nociception [13].

This enhanced anti-nociception led us to hypothesize that spinal Hsp90 inhibitor treatment could be used to improve the therapeutic index of opioids and enable a dose-reduction strategy. This is because many side effects are regulated outside the spinal cord, and would presumably not be impacted by spinal inhibition (e.g. reward in ventral tegmental area and striatum [30], constipation in the gut [37]). If anti-nociception were improved but side effects were either improved or not altered, then a lower dose of opioid could be given in combination with Hsp90 inhibitor treatment. This would hypothetically result in improved or maintained anti-nociception with decreased side effects (see [18] for a parallel approach). A novel dose-reduction strategy of this kind could be used to improve opioid therapy in chronic pain patients, decreasing the impact of the negative side effects of opioid therapy.

Methods

Drugs

KU-32 was synthesized, purified, and characterized as in our previously published work (Compound A4 in [8]). Purity was confirmed by HPLC (>95%) and identity confirmed by HRMS and NMR. KU-32 was stored under desiccation at -20°C, and stock solutions were prepared in DMSO, and also stored at -20°C. A matched Vehicle control for 0.01 nmol KU-32 was included in every experiment, consisting of 0.02% DMSO in sterile USP water. Morphine sulfate pentahydrate was obtained from the NIDA Drug Supply Program, stored at room temperature, and working solutions were made fresh prior to every experiment in sterile USP saline. USP saline injected controls were used for the reward and constipation assays below.

Mice

Male and female CD-1 mice in age-matched cohorts from 5–8 weeks of age were used for all behavioral experiments and were obtained from Charles River Laboratories (Wilmington, MA). CD-1 (a.k.a. ICR) mice are commonly used in opioid research as a line with a strong response to opioid drugs (*e.g.* [2], and our own previous Hsp90 research [13; 22; 24; 33]). Mice were recovered for a minimum of 5 days after shipment before being used in experiments. Mice were housed no more than 5 mice per cage and kept in an AAALAC-accredited vivarium at the University of Arizona under temperature control and 12-h light/dark cycles. All mice were provided with standard lab chow and water available *ad libitum*. The animals were monitored daily, including after surgical procedures, by trained veterinary staff. All experiments performed were in accordance with IACUC-approved protocols at the University of Arizona and by the guidelines of the NIH Guide for the Care and Use of Laboratory Animals. We also adhered to the guidelines of ARRIVE; no adverse events were noted for any of the animals.

Behavioral experiments

All animals were randomized to treatment groups of equal size; the few cases of unequal sample sizes between treatments were due to mouse death during the protocol. This was done by random assignment of mice in one cohort to cages, followed by random block assignment of cages to treatment group. Group sizes were based on previous published work from our lab using these assays [12; 13; 22; 23]. The mice were not habituated to handling. Prior to any behavioral experiment or testing, animals were brought to the testing room in their home cages for at least 1 h for acclimation. Testing always occurred within the same approximate time of day between experiments during the animal light (inactive) cycle, and environmental factors (noise, personnel, and scents) were minimized. All testing apparatus (cylinders, grid boxes, etc.) were cleaned between uses using 70% ethanol and allowed to dry. The experimenter was blinded to treatment group by another laboratory member delivering coded drug vials, which were then decoded after collection of all data. Naïve mice were used for every experiment, including each dose.

Paw incision and mechanical allodynia

Mechanical thresholds were determined prior to surgery using calibrated von Frey filaments (Ugo Basile, Varese, Italy) with the up-down method and four measurements after the first response per mouse as in [9] and our previously published work (e.g. [25]). The mice were housed in a homemade apparatus with Plexiglas walls and ceiling and a wire mesh floor (3-inch wide 4-inch long 3-inch high with 0.25-inch wire mesh). The surgery was then performed by anesthesia with ~2% isoflurane in standard air, preparation of the left plantar hind paw with iodine and 70% ethanol, and a 5-mm incision made through the skin and fascia with a no. 11 scalpel. The muscle was elevated with curved forceps leaving the origin and insertion intact, and the muscle was split lengthwise using the scalpel. The wound was then closed with 5-0 polyglycolic acid sutures. Mice were then injected by the intrathecal (i.t.) route with KU-32 or Vehicle control and left to recover for 24 h. Our i.t. injection protocol is reported in [24]; briefly, the injection was made in awake and restrained animals with a 10 µL Hamilton syringe and 30 g needle (5-7 µL volume) between the L5-L6 vertebrae at a 45° angle, with placement validated by tail twitch. Since the injection was made through skin with no incision or other surgical intervention, repeated injection protocols were performed the same way. The next day, the mechanical threshold was again determined as described above. Mice were then injected with 0.32-5.6 mg/kg morphine by the subcutaneous (s.c.) route, and mechanical thresholds were determined over a 3-hour time course. No animals were excluded from these studies.

Tail-flick assay

Pre-injection tail-flick baselines were determined in a 52°C tail-flick assay with a 10-s cutoff time (method also reported in [24]). The mice were then injected i.t. with KU-32 or Vehicle control with a 24-hour treatment time. 24-hours post-injection baselines were determined. The mice were then injected s.c. with 1, 3.2, 5.6, or 10 mg/kg of morphine, and tail-flick latencies were determined over a 2-hour time course. For tolerance studies, baseline tail flick latencies were taken, and mice were then injected with i.t. with KU-32 or Vehicle control with a 24-hour treatment time. 24 hours later mice were baselined again and then injected with 10 mg/kg s.c. morphine with one tail flick latency measured at 30 minutes post morphine. Mice were injected again with i.t. KU-32 and the process was repeated for an additional 7 days with twice daily morphine injection, and tail flick response measured after the morning injection. No animals were excluded from these studies.

HIV peripheral neuropathy

Mechanical threshold baselines were measured prior to any treatment on the left hind paw using von Frey filaments. HIV peripheral neuropathy was induced by intrathecal injection of gp120 IIIb protein (SPEED BioSystems, Gaithersburg, MD, Cat# YCP1549, 15 ng/µl in 0.1 M PBS and 0.1% BSA, 7-µl volume) using our previously established protocol [24] on days 1, 3, and 5. On day 20 a second mechanical threshold baseline was measured on the left hind paw using von Frey filaments and then KU-32 or Vehicle was injected i.t with a 24-h

treatment time. A third mechanical threshold was then measured on day 21 and morphine (0.32-10 mg/kg s.c.) was then injected, and mechanical thresholds were measured over a time course on the left hind paw. No animals were excluded from these studies.

Conditioned place preference

Conditioned place preference training, baseline runs, and post-training runs were all performed in Spatial Place Preference LE 896/898 rigs (Harvard Apparatus, Holliston, MA). Rigs were designed to consist of two chambers with one connecting chamber. Of the two conditioned chambers, one consisted of black and grey dotted walls with a textured floor. The other chamber consisted of black and grey striped walls with smooth floor. Chamber floors connected to a pressure sensor which transferred ongoing data to a computer running PPC WIN 2.0 software (Harvard Apparatus). Prior to preference training baselines were taken on day 0. Mice were placed in CPP chambers and allowed to roam freely for 15 minutes at ~7am. Chambers were cleaned thoroughly with VersaClean and allowed to dry in-between mice. Mice were then injected with i.t. KU-32 or Vehicle with a 24-hour treatment time. On day 1 mice were injected with i.t. KU-32 or Vehicle again and allowed to recover for 30 minutes. Mice were then injected s.c. with saline or morphine (3.2, 5.6, or 10mg/kg) at ~7am and placed in either stripe or dotted chambers. Half of each group paired morphine with the striped chamber and the other half to the dotted chamber in an unbiased design. At ~12pm mice were then given a second injection of either saline or morphine which was paired to the opposite chamber. This training process was repeated for 4 days total with morning and noon pairings alternating each day. On day 5 mice were placed in CPP chambers and allowed to roam freely for 15 minutes at ~7am. Raw data in the form of seconds and percentage spent in each chamber was exported from PPC WIN 2.0 as an excel file and transferred to GraphPad Prism 8.2 (San Diego, CA) for further analysis.

Opioid induced constipation

Prior to the experiment mice were injected with either KU-32 or Vehicle i.t. and allowed to recover for 24 hours. Morphine (1, 3.2, or 10mg/kg s.c.) or saline was injected and followed by a 6-hour fecal production time course. During this time course the mice were housed in the von Frey boxes used to collect the paw incision and HIV neuropathy data above, which have a grate above a collection plate. The feces were counted and weighed in 1-hour bins and used to construct a cumulative plot. Morphine treated groups were normalized to saline groups and represented as a percentage at each timepoint.

Statistical analysis

All data were reported as the mean ± SEM and normalized where appropriate as described above. The behavioral data from each individual dose was reported raw without maximum possible effect (MPE) or other normalization. Data for dose/response curves (except CPP) was normalized to %MPE using peak effect, except

for constipation, which used Area Under the Curve [MPE = (Response-Baseline) / (Threshold – Baseline) * 100]. The CPP dose/response curve was reported as the % Difference Score [Diff Score = % in Paired - % in Unpaired]. Technical replicates and further details are described in the Figure Legends. Potency (A_{50}) values were calculated by linear regression using our previously reported method [24], with further details in the Figure Legends, and were reported with 95% confidence intervals. Statistical comparisons of individual dose/response curve time courses were performed using Repeated Measures 2-Way ANOVA with Sidak's (tail flick, paw incision, HIV neuropathy, tolerance rescue, constipation) or Tukey's (tolerance, CPP) *post hoc* tests. The Geisser-Greenhouse correction was used to account for a potential lack of sphericity of the data, permitting valid Repeated Measures ANOVA. ANOVA *post hoc* tests were only performed when ANOVA F values indicated a significant difference, and there was homogeneity of variance (permitting parametric analysis). In all cases, significance was defined as $p < 0.05$, and statistical analysis was only performed for groups of $N \geq 5$. The group sizes reported represent independent individual mice tested in each assay. All graphing and statistical analyses were performed using GraphPad Prism 8.2. Approximately equal numbers of male and female mice were used for each experiment. Comparison by 2 Way ANOVA using sex as a variable revealed no sex differences in this study, so all male and female mice were combined.

Results

Spinal Hsp90 inhibition enhances morphine anti-nociception in multiple pain models

Based on our earlier work [13] we hypothesized that spinal cord Hsp90 inhibition would consistently enhance morphine anti-nociception over a full dose range in different acute and chronic pain models. We tested this using male and female CD-1 mice injected with 0.01 nmol of the non-isoform-selective Hsp90 inhibitor KU-32 or Vehicle control by the i.t. route with a default treatment time of 24 hours (time point based on our earlier work [13; 22; 24; 33]). After the 24 hour treatment time, the mice were treated with a dose range of morphine and anti-nociception was measured.

We first tested acute thermal nociception in uninjured mice using the well-established tail flick model. KU-32 treatment caused a consistent and significant elevation in morphine anti-nociception over the dose range of 1-5.6 mg/kg (**Figure 1A-C**; all ANOVA F values reported in **Table 1**). The response was not different at 10 mg/kg; however, 10 mg/kg is a maximal dose in this assay, and responses were not recorded past the 10 second threshold (**Figure 1D**). Dose/response analysis revealed a potency of 3.0 (2.5 – 3.7; 95% confidence intervals reported in parentheses) mg/kg in Vehicle treated mice and 1.6 (1.3 – 2.0) mg/kg in KU-32 treated mice, representing a 1.9 fold shift improvement in potency (**Figure 1E**).

This result was encouraging; however, tail flick is a spinal reflex in uninjured animals, and may not translate to clinical pain conditions. We thus used the post-surgical paw incision assay to model post-surgical

pain, a common opioid indication [5]. Much as in heat-induced tail flick, KU-32 caused a significant and consistent elevation in morphine anti-nociception over the 0.32 – 5.6 mg/kg dose range (**Figure 2A-E**). Dose/response analysis showed an A_{50} potency value of 2.4 (2.0 – 2.8) mg/kg for Vehicle animals and 0.85 (0.64 – 1.1) mg/kg for KU-32 animals, representing a 2.8 fold improvement in potency (**Figure 2F**).

These results are again promising, but both pain states are acute and short in duration, and do not represent chronic pain, which is the most difficult to treat in the clinic. We thus used the HIV peripheral neuropathy model induced by gp120 protein injection, which is a sustained and long-lasting neuropathic pain model [42]. After 3 sustained weeks of chronic pain, the mice were treated with KU-32 or Vehicle control and tested as above. Again, KU-32 treatment caused a sustained and significant increase in morphine anti-nociception over the 0.32-10 mg/kg dose range (**Figure 3A-E**). Dose/response analysis showed a potency of 4.2 (3.7 – 4.8) mg/kg for Vehicle treatment and 1.2 (0.87 – 1.5) mg/kg for KU-32 treatment, an improvement of 3.5 fold (**Figure 3F**). Not only did KU-32 improve opioid anti-nociception in this chronic pain model, it had the largest fold-shift improvement of the 3 models tested. Importantly, KU-32 treatment did not cause baseline differences in any pain state measured.

Spinal Hsp90 inhibition reduces morphine tolerance and rescues established tolerance

The results above support our hypothesis that spinal Hsp90 inhibition could make opioids more potent. However, at the same time, if side effect potencies are enhanced, then the improvement does not result in an improved therapeutic index or improved opioid therapy. We thus tested the potency of morphine side effects with spinal Hsp90 inhibitor treatment, beginning with anti-nociceptive tolerance. Over a 7-day repeated treatment period, the anti-nociceptive efficacy of morphine steadily decreased in Vehicle treated mice, resulting in a complete loss of anti-nociceptive efficacy by day 7 for the entire 1-10 mg/kg dose range (**Figure 4A-C**). In contrast, KU-32 treatment caused a significant decrease in tolerance over the full 7 day treatment period and full dose range, so that at least some significant anti-nociceptive efficacy remained by day 7 at each dose with KU-32 treatment (**Figure 4A-C**). Notably, baseline responses were not altered by any treatment, demonstrating that KU-32 treatment is not altering baseline nociception (**Figure 4A-C**). To quantify this result, we compared day 1 vs. day 4 responses for each dose and treatment; day 4 was chosen because days 5-7 have no quantifiable Vehicle response for at least one dose each. Dose/response analysis of these data revealed a 21 fold tolerance shift from day 1 to day 4 for Vehicle-treated mice; this tolerance shift was reduced to 2.9 fold in KU-32 treated mice (**Figure 4D**).

This result suggests that morphine tolerance is blocked by KU-32 treatment; however, KU-32 treatment began before the tolerance regimen and continued during every morphine injection. We thus sought to determine if KU-32 treatment would reverse already-established tolerance. We thus subjected naïve mice to a tolerance regimen as above for 3 days; all mice showed normal morphine anti-nociception on day 1 and a near-complete

tolerance by day 3 (**Figure 5A**). We then injected these mice with KU-32 or Vehicle, and 24 hours later, injected morphine again. The Vehicle-treated mice showed little anti-nociception, showing how their tolerance was maintained (**Figure 5B**). In sharp contrast, the KU-32 treated mice showed a full anti-nociceptive response to morphine, comparable to their day 1 response (**Figure 5B**). These results suggest that not only can spinal Hsp90 inhibition reduce the development of tolerance, it can restore responsiveness to already-tolerant mice.

Spinal Hsp90 inhibition does not alter morphine-induced constipation and reward

Based on our rationale above, we continued to investigate clinically-relevant opioid side effects. Opioid-induced constipation is a highly clinically significant side effect, that lowers medication compliance and patient quality of life [37]. After KU-32 or Vehicle treatment, we injected a dose-range of morphine and measured fecal output over a 6 hour time course. Compared to saline injected controls, morphine caused ~40% constipation at 1 mg/kg, that plateaued at ~70% constipation at 3.2-10 mg/kg (**Figure 6A-D**). Vehicle vs. KU-32 saline or morphine treatment curves were not significantly different at any dose or time point. After normalizing each treatment group to saline-injected controls, dose/response analysis revealed overlapping curves with a constipation potency of 0.67 (0.32 – 0.94) mg/kg for Vehicle and 0.97 (0.59 – 1.3) mg/kg for KU-32, further supporting the conclusion that KU-32 treatment did not alter morphine constipation (**Figure 6D**).

We next tested opioid-induced reward, which is the basis for opioid addiction, and has contributed to an opioid abuse and overdose crisis [30; 40]. We used the well-established conditioned place preference (CPP) assay, which demonstrates reward (or aversion) learning [12]. Over the 3.2-10 mg/kg morphine dose range, we observed an increasing preference for the morphine-paired chamber by Vehicle-treated mice, that rose to the level of significance at 10 mg/kg of morphine (**Figure 7A-C**). KU-32 treatment did not differ significantly from Vehicle treatment at any dose, and also showed significant preference at 10 mg/kg of morphine (**Figure 7A-C**). Dose/response analysis showed overlapping curves and a potency of 5.1 (2.7 – 7.7) mg/kg for Vehicle and 5.3 (-∞ - +∞) mg/kg for KU-32, further supporting a lack of effect of KU-32 treatment on morphine-induced reward learning (**Figure 7D**).

Discussion

In this study, we observed that inhibition of spinal cord Hsp90 improved the therapeutic index of morphine. Morphine anti-nociceptive potency was consistently increased by 2-4 fold in multiple acute and chronic pain models; at the same time, anti-nociceptive tolerance was reduced, established tolerance could be rescued, and constipation and reward were not altered. These results suggest that with spinal Hsp90 inhibition, a lower dose of opioid could be given in the clinic, which would result in a maintained (or improved) anti-nociception/analgesia, due to anti-nociceptive potentiation. However, since side effects are improved or not

altered, this lower dose of morphine should result in a lower side effect burden. Our earlier work suggests that other opioids, specifically oxymorphone, are regulated similarly by Hsp90 inhibition as morphine, albeit in different pain models and inhibitor route [33]. This suggests that a broad spectrum of opioid drugs could be improved. Such a dose-reduction strategy using Hsp90 inhibitors represents a completely novel approach to improve opioid therapy and reduce side effects. A cautionary note should be made, however; this is early stage research, and we have not yet tested the impact of spinal Hsp90 inhibition on opioid-induced respiratory depression, the most important safety-related side effect. Further study will thus be required to determine if this is a viable strategy for clinical translation.

Selectively boosting anti-nociceptive potency/efficacy in order to enable a dose-reduction strategy has precedent in the literature. Examples include demonstrated synergy between the cannabinoid receptor type 2 and opioid receptor for anti-nociception, without synergizing the side effects of either [18]. Further examples include selective inhibition of Gβγ signaling downstream of the mu opioid receptor, which similarly potentiates anti-nociception but not side effects [19], morphine and clonidine synergy [34], and using chemokine receptor antagonists to enable opioid dose-reduction [14]. These examples provide precedent and a reason to believe that dose-reduction with Hsp90 inhibitors would work. At the same time, to our knowledge, no such approaches are being used in the clinic, providing novelty and opportunity to use our findings.

One potential limitation to our findings is the need to inject the Hsp90 inhibitors intrathecally. Indeed, in our earlier study, we showed that systemic non-selective Hsp90 inhibitors recapitulated brain inhibition, resulting in less anti-nociception [13]. For the greatest impact, we will need to find a way to circumvent this limitation. One potential avenue is to investigate specific Hsp90 isoforms and co-chaperones active in the spinal cord. In our earlier work, we found that the Hsp90α isoform and the co-chaperones p23 and Cdc37 were responsible for regulating anti-nociception in the brain [22]. If different isoforms and/or co-chaperones regulate opioid anti-nociception in the spinal cord, then we could use isoform- and co-chaperone-selective inhibitors to selectively inhibit spinal cord Hsp90 even with systemic administration. Such inhibitors have been developed, including inhibitors selective for each isoform, and co-chaperone inhibitors like gedunin and celastrol [7; 10; 33; 44]. Such a difference is reasonable, considering the very different mechanisms and opioid responses we've observed when comparing brain to spinal cord Hsp90 [13; 24]. However, even if this difficulty cannot be circumvented, there is still a considerable patient population that uses intrathecal drug delivery, including opioids, the anti-nociceptive peptide Prialt, and other medications [11; 32]. Such a population could benefit from intrathecal delivery of non-selective Hsp90 inhibitors as we've shown here.

Another potential barrier to translation could be side effects induced by the Hsp90 inhibitor treatment. It is true that first generation Hsp90 inhibitors like 17-AAG failed clinical trials due to liver toxicity [31]. However, later generation compounds like CNF2024 were far better tolerated, suggesting this toxicity could be off-target

rather than Hsp90-mediated [31]. Further supporting potential clinical use, the compound in this study, KU-32, was shown to be neuroprotective, and a derivative KU-596 is currently in clinical trials for diabetic neuropathy management [38; 39]. Another potential means to reduce side effects could be the development of the isoform-selective inhibitors mentioned above. Since each isoform is expressed in different parts of the cell and engages a unique client protein complement, selectively targeting one isoform should produce less adverse effects than targeting all. An analogous approach has been used for the closely related Hsp70 [4].

These observations also raise the question of by what mechanism are these effects taking place. Our earlier work described an ERK-RSK kinase cascade that is not normally active in spinal cord, but becomes "unchained" with Hsp90 inhibition and promotes enhanced anti-nociception [13]. This cascade is presumably responsible for the wider enhancement in anti-nociceptive potency we see here across multiple acute and chronic pain models. At the same time, reward is primarily modulated by a ventral tegmental area-striatal circuit [30] among other forebrain circuits, while constipation is primarily modulated by opioid receptors in the gut [37]; it thus makes sense why local spinal inhibition would not impact these regions and change the potency of those side effects. This leaves tolerance. Several studies have found that spinal circuits modulate opioid tolerance through various mechanisms, suggesting that local spinal inhibition could alter tolerance [41; 43]. Spinal Hsp90 inhibition may favorably alter these mechanisms, blocking tolerance. Similarly, Hsp90 inhibition has been shown to be anti-inflammatory, and spinal neuroinflammation has been shown to contribute to opioid tolerance [26; 28]. Alternately, enhanced anti-nociceptive efficacy could lead to less tolerance over time simply because the efficacy was higher to begin with; in support of this hypothesis, high efficacy opioid agonists have been shown to produce slower/less tolerance than low efficacy agonists [29].

However, these hypotheses only address the slower tolerance seen over time with repeated treatment, they do not explain the tolerance rescue we observed. One potential clue for this rescue mechanism could be our earlier findings that both brain and spinal cord effects of Hsp90 inhibition on anti-nociception require rapid protein translation [13; 22; 33]. The translation inhibitor we used had no impact on anti-nociception in Vehicle-treated mice, suggesting that this mechanism is newly activated upon Hsp90 inhibitor treatment. The mechanisms we are uncovering could thus be parallel pathways to the normal/baseline anti-nociceptive signaling, which is further supported by our work on the spinal ERK-RSK cascade [13]. In the case of the tolerance rescue, we could be observing new pathways becoming turned on that have not developed tolerance as have the normal/baseline pathways. These new pathways could thus provide anti-nociceptive responsiveness even when other parts of the system remain tolerant. It's also unclear at this point whether the tolerance reduction and the tolerance rescue share the same or different mechanisms. These questions will provide new basic science directions to follow while at the same time these findings can be used to inform a new clinical dose-reduction approach.

Author Contributions

DID performed most mouse experiments, analyzed most of the data, and collaborated on experimental and project design. KAG, JLB, and CSC performed some mouse experiments and analyzed some of the data. SM synthesized and purified the Hsp90 inhibitor KU-32 used throughout the project. BSJB supervised and trained SM in the synthesis of KU-32. JMS conceived the initial idea for the project, collaborated on experimental and project design, analyzed some of the data, and wrote the manuscript. All authors had editorial input into the manuscript.

Acknowledgments

We would like to acknowledge Drs. Tally Largent-Milnes and Todd Vanderah at the University of Arizona for the use of their conditoned place preference equipment and expertise. This work was supported by an Arizona Biomedical Research Commission New Investigator Award #ADHS18-198875 and institutional funds from the University of Arizona, both to JMS. The work was also supported by NIH grants R01CA213566 and R01NS075311 to BSJB. JMS is an equity holder in *Teleport Pharmaceuticals, LLC* and *Botanical Results, LLC*, but these companies are not Hsp90-related. The authors have no other relevant conflicts to declare.

References

[1] Abul-Husn NS, Annangudi SP, Ma'ayan A, Ramos-Ortolaza DL, Stockton SD, Jr., Gomes I, Sweedler JV, Devi LA. Chronic morphine alters the presynaptic protein profile: identification of novel molecular targets using proteomics and network analysis. PloS one 2011;6(10):e25535.

[2] Ananthan S, Saini SK, Dersch CM, Xu H, McGlinchey N, Giuvelis D, Bilsky EJ, Rothman RB. 14-Alkoxy- and 14-acyloxypyridomorphinans: mu agonist/delta antagonist opioid analgesics with diminished tolerance and dependence side effects. J Med Chem 2012;55(19):8350-8363.

[3] Annemans L. Pharmacoeconomic impact of adverse events of long-term opioid treatment for the management of persistent pain. Clinical drug investigation 2011;31(2):73-86.

[4] Assimon VA, Gillies AT, Rauch JN, Gestwicki JE. Hsp70 protein complexes as drug targets. Current pharmaceutical design 2013;19(3):404-417.

[5] Berge OG. Predictive validity of behavioural animal models for chronic pain. Br J Pharmacol 2011;164(4):1195-1206.

[6] Berthelot JM, Darrieutort-Lafitte C, Le Goff B, Maugars Y. Strong opioids for noncancer pain due to musculoskeletal diseases: Not more effective than acetaminophen or NSAIDs. Joint Bone Spine 2015;82(6):397-401.

[7] Brandt GE, Schmidt MD, Prisinzano TE, Blagg BS. Gedunin, a novel hsp90 inhibitor: semisynthesis of derivatives and preliminary structure-activity relationships. J Med Chem 2008;51(20):6495-6502.

[8] Burlison JA, Neckers L, Smith AB, Maxwell A, Blagg BS. Novobiocin: redesigning a DNA gyrase inhibitor for selective inhibition of hsp90. J Am Chem Soc 2006;128(48):15529-15536.

[9] Chaplan SR, Bach FW, Pogrel JW, Chung JM, Yaksh TL. Quantitative assessment of tactile allodynia in the rat paw. J Neurosci Methods 1994;53(1):55-63.

[10] Crowley VM, Huard DJE, Lieberman RL, Blagg BSJ. Second Generation Grp94-Selective Inhibitors Provide Opportunities for the Inhibition of Metastatic Cancer. Chemistry 2017;23(62):15775-15782.

[11] Duggan PJ, Tuck KL. Bioactive Mimetics of Conotoxins and other Venom Peptides. Toxins (Basel) 2015;7(10):4175-4198.

[12] Duron DI, Hanak F, Streicher JM. Daily intermittent fasting in mice enhances morphine-induced anti-nociception while mitigating reward, tolerance, and constipation. Pain 2020.

[13] Duron DI, Lei W, Barker NK, Stine C, Mishra S, Blagg BSJ, Langlais PR, Streicher JM. Inhibition of Hsp90 in the spinal cord enhances the antinociceptive effects of morphine by activating an ERK-RSK pathway. Sci Signal 2020;13(630).

[14] Eisenstein TK, Chen X, Inan S, Meissler JJ, Tallarida CS, Geller EB, Rawls SM, Cowan A, Adler MW. Chemokine Receptor Antagonists in Combination with Morphine as a Novel Strategy for Opioid Dose Reduction in Pain Management. Mil Med 2020;185(Suppl 1):130-135.

[15] Finnerup NB, Attal N, Haroutounian S, McNicol E, Baron R, Dworkin RH, Gilron I, Haanpaa M, Hansson P, Jensen TS, Kamerman PR, Lund K, Moore A, Raja SN, Rice AS, Rowbotham M, Sena E, Siddall P, Smith BH, Wallace M. Pharmacotherapy for neuropathic pain in adults: a systematic review and meta-analysis. Lancet Neurol 2015;14(2):162-173.

[16] Gaskin DJ, Richard P. The economic costs of pain in the United States. J Pain 2012;13(8):715-724.

[17] Grace PM, Strand KA, Galer EL, Rice KC, Maier SF, Watkins LR. Protraction of neuropathic pain by morphine is mediated by spinal damage associated molecular patterns (DAMPs) in male rats. Brain Behav Immun 2017.

[18] Grenald SA, Young MA, Wang Y, Ossipov MH, Ibrahim MM, Largent-Milnes TM, Vanderah TW. Synergistic attenuation of chronic pain using mu opioid and cannabinoid receptor 2 agonists. Neuropharmacology 2017;116:59-70.

[19] Hoot MR, Sypek EI, Reilley KJ, Carey AN, Bidlack JM, McLaughlin JP. Inhibition of Gbetagamma-subunit signaling potentiates morphine-induced antinociception but not respiratory depression, constipation, locomotion, and reward. Behav Pharmacol 2013;24(2):144-152.

[20] Hutchinson MR, Ramos KM, Loram LC, Wieseler J, Sholar PW, Kearney JJ, Lewis MT, Crysdale NY, Zhang Y, Harrison JA, Maier SF, Rice KC, Watkins LR. Evidence for a role of heat shock protein-90 in toll like receptor 4 mediated pain enhancement in rats. Neuroscience 2009;164(4):1821-1832.

[21] Koshimizu TA, Tsuchiya H, Tsuda H, Fujiwara Y, Shibata K, Hirasawa A, Tsujimoto G, Fujimura A. Inhibition of heat shock protein 90 attenuates adenylate cyclase sensitization after chronic morphine treatment. Biochemical and biophysical research communications 2010;392(4):603-607.

[22] Lei W, Duron DI, Stine C, Mishra S, Blagg BSJ, Streicher JM. The Alpha Isoform of Heat Shock Protein 90 and the Co-chaperones p23 and Cdc37 Promote Opioid Anti-nociception in the Brain. Front Mol Neurosci 2019;12:294.

[23] Lei W, Mullen N, McCarthy S, Brann C, Richard P, Cormier J, Edwards K, Bilsky EJ, Streicher JM. Heat-shock protein 90 (Hsp90) promotes opioid-induced anti-nociception by an ERK mitogen-activated protein kinase (MAPK) mechanism in mouse brain. J Biol Chem 2017;292(25):10414-10428.

[24] Lei W, Mullen N, McCarthy S, Brann C, Richard P, Cormier J, Edwards K, Bilsky EJ, Streicher JM. Heat shock protein 90 (Hsp90) promotes opioid-induced anti-nociception by an ERK Mitogen Activated Protein Kinase (MAPK) mechanism in mouse brain. J Biol Chem 2017.

[25] Lei W, Vekariya RH, Ananthan S, Streicher JM. A Novel Mu-Delta Opioid Agonist Demonstrates Enhanced Efficacy with Reduced Tolerance and Dependence in Mouse Neuropathic Pain Models. J Pain 2019.

[26] Lewis SS, Hutchinson MR, Rezvani N, Loram LC, Zhang Y, Maier SF, Rice KC, Watkins LR. Evidence that intrathecal morphine-3-glucuronide may cause pain enhancement via toll-like receptor 4/MD-2 and interleukin-1beta. Neuroscience 2010;165(2):569-583.

[27] Li J, Buchner J. Structure, function and regulation of the hsp90 machinery. Biomedical journal 2013;36(3):106-117.

[28] Pan Y, Sun X, Jiang L, Hu L, Kong H, Han Y, Qian C, Song C, Qian Y, Liu W. Metformin reduces morphine tolerance by inhibiting microglial-mediated neuroinflammation. J Neuroinflammation 2016;13(1):294.

[29] Pawar M, Kumar P, Sunkaraneni S, Sirohi S, Walker EA, Yoburn BC. Opioid agonist efficacy predicts the magnitude of tolerance and the regulation of mu-opioid receptors and dynamin-2. Eur J Pharmacol 2007;563(1-3):92-101.

[30] Sandweiss AJ, McIntosh MI, Moutal A, Davidson-Knapp R, Hu J, Giri AK, Yamamoto T, Hruby VJ, Khanna R, Largent-Milnes TM, Vanderah TW. Genetic and pharmacological antagonism of NK1 receptor prevents opiate abuse potential. Mol Psychiatry 2017.

[31] Sidera K, Patsavoudi E. HSP90 inhibitors: current development and potential in cancer therapy. Recent Pat Anticancer Drug Discov 2014;9(1):1-20.

[32] Sindt JE, Odell DW, Dalley AP, Brogan SE. Initiation of Intrathecal Drug Delivery Dramatically Reduces Systemic Opioid Use in Patients With Advanced Cancer. Neuromodulation 2020.

[33] Stine C, Coleman DL, Flohrschutz AT, Thompson AL, Mishra S, Blagg BS, Largent-Milnes TM, Lei W, Streicher JM. Heat shock protein 90 inhibitors block the anti-nociceptive effects of opioids in mouse chemotherapy-induced neuropathy and cancer bone pain models. Pain 2020.

[34] Stone LS, German JP, Kitto KF, Fairbanks CA, Wilcox GL. Morphine and clonidine combination therapy improves therapeutic window in mice: synergy in antinociceptive but not in sedative or cardiovascular effects. PloS one 2014;9(10):e109903.

[35] Streicher JM. The role of heat shock protein 90 in regulating pain, opioid signaling, and opioid antinociception. Vitam Horm 2019;111:91-103.

[36] Streicher JM. The Role of Heat Shock Proteins in Regulating Receptor Signal Transduction. Mol Pharmacol 2019;95(5):468-474.

[37] Streicher JM, Bilsky EJ. Peripherally Acting micro-Opioid Receptor Antagonists for the Treatment of Opioid-Related Side Effects: Mechanism of Action and Clinical Implications. J Pharm Pract 2017:897190017732263.

[38] Urban MJ, Li C, Yu C, Lu Y, Krise JM, McIntosh MP, Rajewski RA, Blagg BS, Dobrowsky RT. Inhibiting heat-shock protein 90 reverses sensory hypoalgesia in diabetic mice. ASN neuro 2010;2(4):e00040.

[39] Urban MJ, Pan P, Farmer KL, Zhao H, Blagg BS, Dobrowsky RT. Modulating molecular chaperones improves sensory fiber recovery and mitochondrial function in diabetic peripheral neuropathy. Exp Neurol 2012;235(1):388-396.

[40] Warner M, Trinidad JP, Bastian BA, Minino AM, Hedegaard H. Drugs Most Frequently Involved in Drug Overdose Deaths: United States, 2010-2014. Natl Vital Stat Rep 2016;65(10):1-15.

[41] Xu JT, Zhao JY, Zhao X, Ligons D, Tiwari V, Atianjoh FE, Lee CY, Liang L, Zang W, Njoku D, Raja SN, Yaster M, Tao YX. Opioid receptor-triggered spinal mTORC1 activation contributes to morphine tolerance and hyperalgesia. The Journal of clinical investigation 2014.

[42] Yuan SB, Shi Y, Chen J, Zhou X, Li G, Gelman BB, Lisinicchia JG, Carlton SM, Ferguson MR, Tan A, Sarna SK, Tang SJ. Gp120 in the pathogenesis of human immunodeficiency virus-associated pain. Ann Neurol 2014;75(6):837-850.

[43] Zhai ML, Chen Y, Liu C, Wang JB, Yu YH. Spinal glucocorticoid receptorregulated chronic morphine tolerance may be through extracellular signalregulated kinase 1/2. Mol Med Rep 2018;18(1):1074-1080.

[44] Zhang T, Hamza A, Cao X, Wang B, Yu S, Zhan CG, Sun D. A novel Hsp90 inhibitor to disrupt Hsp90/Cdc37 complex against pancreatic cancer cells. Molecular cancer therapeutics 2008;7(1):162-170.

[45] Zhang Y, Zhou P, Wang Z, Chen M, Fu F, Su R. Hsp90beta positively regulates mu-opioid receptor function. Life Sci 2020;252:117676.

Figures

Group	F Values				Residual (DF, SS)
	Subject	Time	Treatment	Time x Treatment	
Tail Fl. – 1	F (18, 144) = 6.0*	F (4.592, 82.65) = 63.7*	F (1, 18) = 8.3*	F (8, 144) = 8.4*	144, 31.3
Tail Fl. – 3.2	F (28, 224) = 8.4*	F (4.244, 118.8) = 156.1*	F (1, 28) = 15.1*	F (8, 224) = 8.3*	224, 126.8
Tail Fl. – 5.6	F (18, 144) = 6.2*	F (3.342, 60.15) = 127.6*	F (1, 18) = 13.0*	F (8, 144) = 7.1*	144, 130.2
Tail Fl. – 10	F (18, 144) = 9.6*	F (3.286, 59.14) = 114.8*	F (1, 18) = 1.9	F (8, 144) = 1.7	144, 169.7
Paw Inc. – 1	F (17, 136) = 2.4*	F (3.662, 62.25) = 64.2*	F (1, 17) = 14.6*	F (8, 136) = 4.8*	136, 14.6
Paw Inc. – 1.8	F (18, 144) = 5.1*	F (3.101, 55.81) = 65.1*	F (1, 18) = 12.7*	F (8, 144) = 6.8*	144, 20.1
Paw Inc. – 3.2	F (18, 144) = 3.7*	F (4.701, 84.62) = 62.2*	F (1, 18) = 26.0*	F (8, 144) = 5.2*	144, 26.6
HIV – 1.8	F (18, 162) = 1.1	F (3.147, 56.64) = 216.5*	F (1, 18) = 42.1*	F (9, 162) = 7.5*	162, 6.9
HIV – 3.2	F (18, 162) = 3.2*	F (3.307, 59.52) = 76.3*	F (1, 18) = 30.2*	F (9, 162) = 13.0*	162, 20.8
HIV – 5.6	F (18, 162) = 3.0*	F (4.112, 74.01) = 85.5*	F (1, 18) = 94.7*	F (9, 162) = 17.2*	162, 19.1
Tol. – 1	F (36, 252) = 6.4*	F (5.424, 195.3) = 53.4*	F (3, 36) = 50.1*	F (21, 252) = 19.5*	252, 30.6
Tol. – 3.2	F (36, 252) = 5.6*	F (4.614, 166.1) = 82.8*	F (3, 36) = 119.4*	F (21, 252) = 24.6*	252, 52.8
Tol. – 10	F (36, 252) = 9.1*	F (4.264, 153.5) = 41.3*	F (3, 36) = 55.3*	F (21, 252) = 18.7*	252, 156.1
Tol. Res. – D1-D3	F (36, 252) = 7.1*	F (5.685, 204.7) = 315.6*	F (3, 36) = 120.7*	F (21, 252) = 44.9*	252, 47.4
Tol. Res. – D4	F (18, 126) = 12.7*	F (3.090, 55.62) = 86.3*	F (1, 18) = 42.1*	F (7, 126) = 30.8*	126, 42.8
Const. – 1	F (56, 280) = 68.7*	F (1.291, 72.30) = 76.0*	F (3, 56) = 2.6	F (15, 280) = 0.96	280, 1.4
Const. – 3.2	F (36, 180) = 33.9*	F (1.516, 54.57) = 28.9*	F (3, 36) = 11.8*	F (15, 180) = 1.2	180, 0.32
Const. – 10	F (36, 180) = 23.3*	F (1.633, 58.80) = 28.8*	F (3, 36) = 8.3*	F (15, 180) = 2.2*	180, 0.5
CPP – 3.2	F (30, 30) = 1.28	F (1, 30) = 0.43	F (1, 30) = 0.008	F (1, 30) = 0.73	30, 2473
CPP – 5.6	F (30, 30) = 1.14	F (1, 30) = 6.6*	F (1, 30) = 0.08	F (1, 30) = 1.3	30, 2511
CPP - 10	F (30, 30) = 1.4	F (1, 30) = 19.5*	F (1, 30) = 0.23	F (1, 30) = 5.8e-6	30, 2137

Table 1: ANOVA F values. All F values with degrees of freedom and residuals for ANOVA analyses reported. * = $p < 0.05$. DF = degrees of freedom; SS = sum of squares.

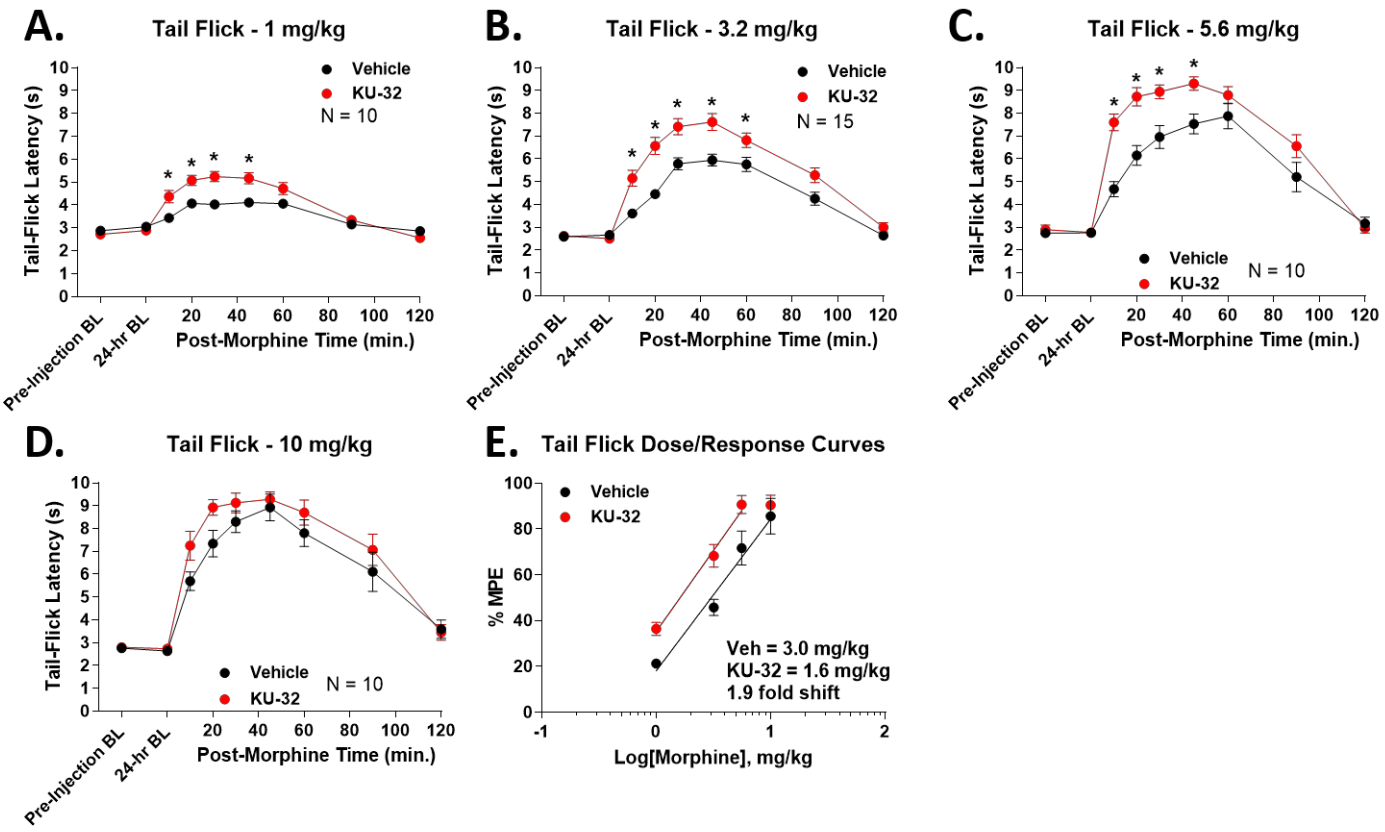

Figure 1: Spinal Hsp90 inhibition increases morphine potency in acute heat-induced tail flick. Male and female CD-1 mice were injected i.t. with 0.01 nmol KU-32 or Vehicle control, 24 hours, then 1-10 mg/kg morphine, s.c.. Tail flick responses were recorded at 52°C with a 10 sec cutoff. Data reported as the mean ± SEM, with sample sizes of mice/group noted in each graph. 2-3 technical replicates were performed per dose. * = $p < 0.05$ vs. same time point Vehicle group by RM 2 Way ANOVA with Sidak's *post hoc* test. **A-D)** Individual dose curves shown as noted. Data not normalized. **E)** Dose/response analysis performed for individual curves, normalized as %MPE (baseline vs. 10 sec cutoff). A_{50}: Vehicle = 3.0 (2.5 – 3.7) mg/kg; KU-32 = 1.6 (1.3 – 2.0) mg/kg; 1.9 fold increase in potency.

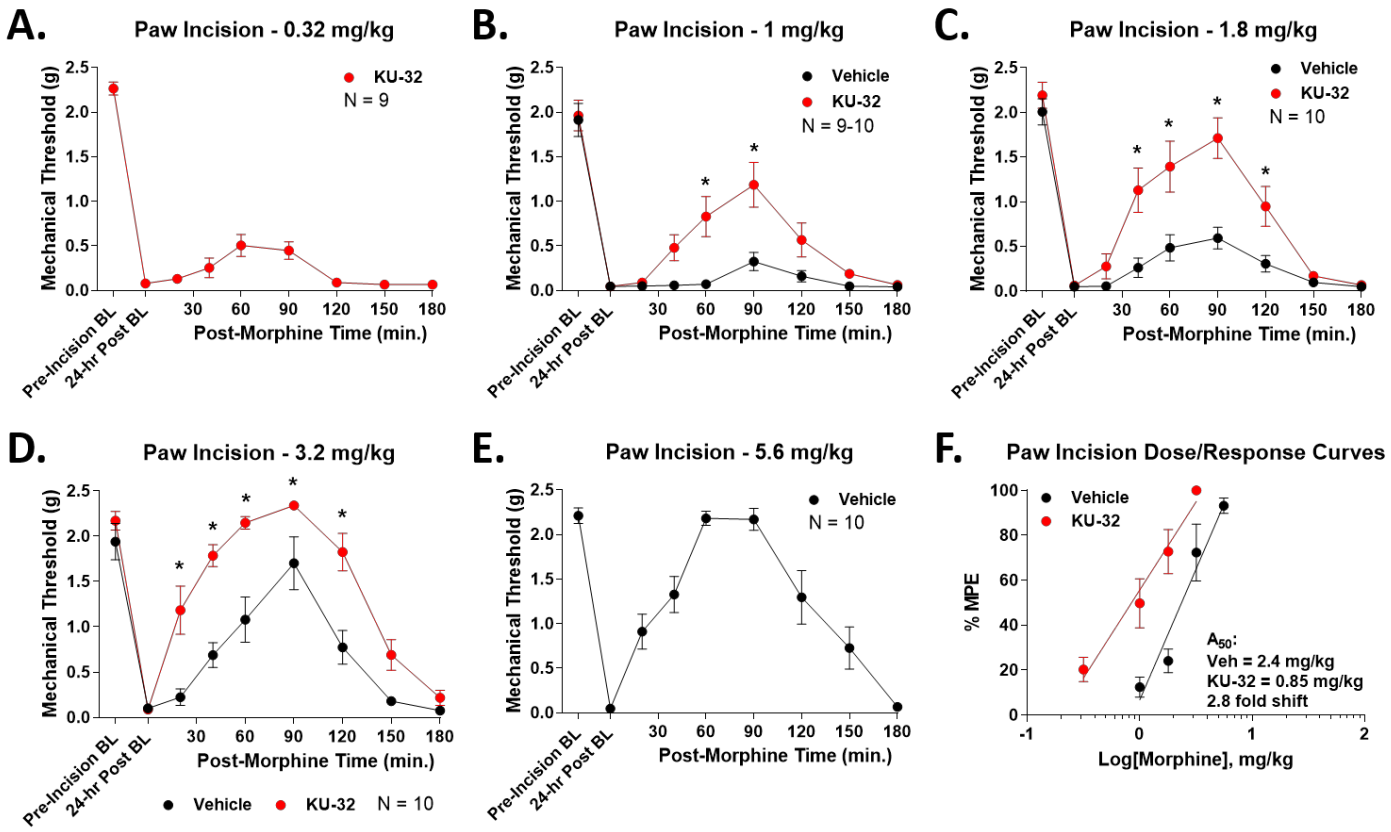

Figure 2: Spinal Hsp90 inhibition increases morphine potency in acute post-surgical paw incision pain. Male and female CD-1 mice had the paw incision surgery performed, then were injected i.t. with 0.01 nmol KU-32 or Vehicle control, 24 hours, then 0.32-5.6 mg/kg morphine, s.c.. Paw withdrawal responses recorded using von Frey filaments, including pre- and post-surgical baselines, validating the pain state. Data reported as the mean ± SEM, with sample sizes of mice/group noted in each graph. 2 technical replicates were performed per dose. * = $p < 0.05$ vs. same time point Vehicle group by RM 2 Way ANOVA with Sidak's *post hoc* test. **A-E)** Individual dose curves shown as noted. Data not normalized. Vehicle at 0.32 mg/kg and KU-32 at 5.6 mg/kg were not measured since these would be too low (Vehicle) or hit the assay threshold (KU-32), meaning they would not fit the linear dose/response model used. **F)** Dose/response analysis performed for individual curves, normalized as %MPE (baseline vs. 2.34 g cutoff). A_{50}: Vehicle = 2.4 (2.0 – 2.8) mg/kg; KU-32 = 0.85 (0.64 – 1.1) mg/kg; 2.8 fold increase in potency.

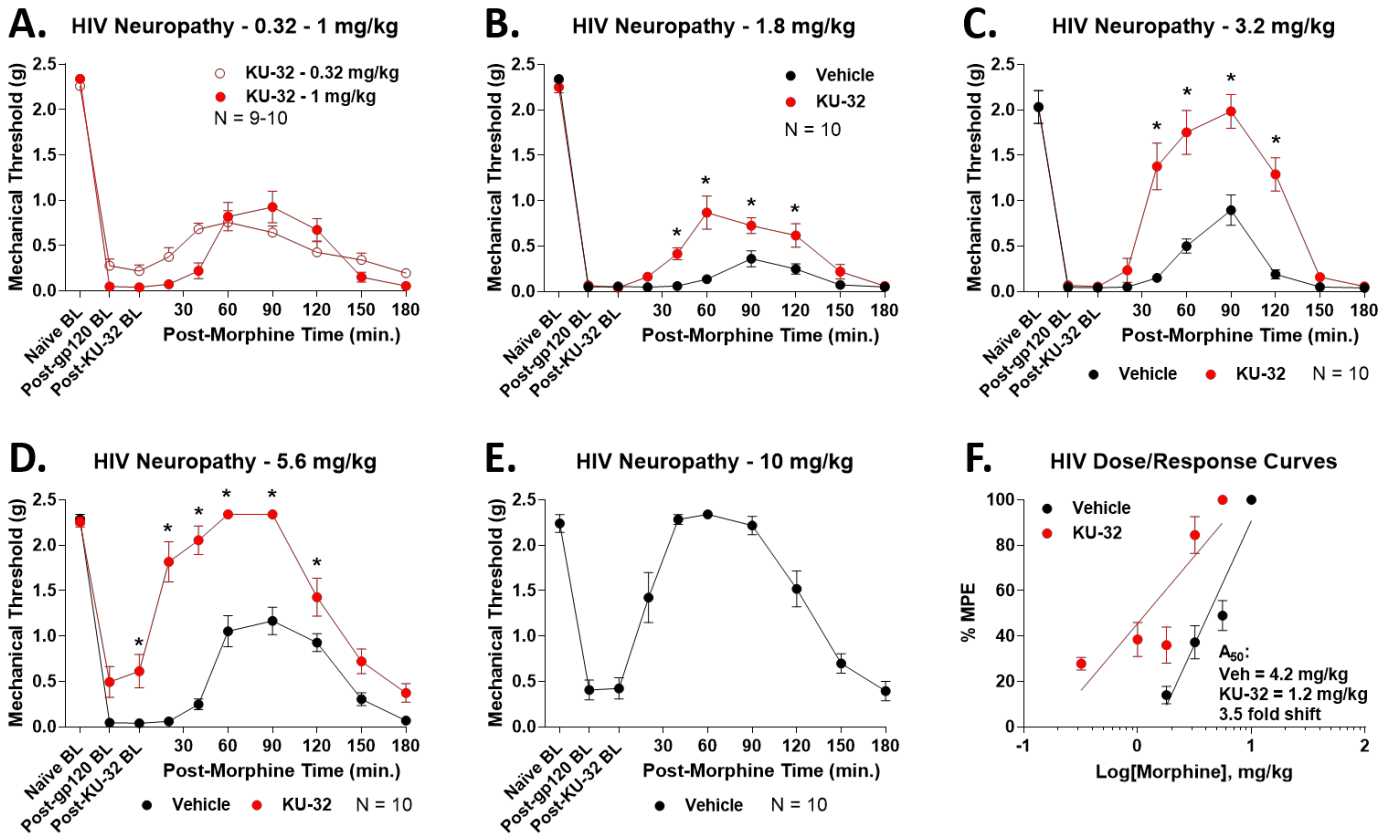

Figure 3: Spinal Hsp90 inhibition increases morphine potency in chronic HIV neuropathy pain. Male and female CD-1 mice were injected i.t. with gp120 protein on days 1, 3, and 5 (see Methods). On day 20, mice were injected i.t. with 0.01 nmol KU-32 or Vehicle control, 24 hours, then 0.32-10 mg/kg morphine, s.c.. Paw withdrawal responses recorded using von Frey filaments, including pre- and post-treatment baselines, validating the pain state. Data reported as the mean ± SEM, with sample sizes of mice/group noted in each graph. 2 technical replicates were performed per dose. * = $p < 0.05$ vs. same time point Vehicle group by RM 2 Way ANOVA with Sidak's *post hoc* test. **A-E)** Individual dose curves shown as noted. Data not normalized. Vehicle at 0.32-1 mg/kg and KU-32 at 10 mg/kg were not measured since these would be too low (Vehicle) or hit the assay threshold (KU-32), meaning they would not fit the linear dose/response model used. **F)** Dose/response analysis performed for individual curves, normalized as %MPE (baseline vs. 2.34 g cutoff). A_{50}: Vehicle = 4.2 (3.7 – 4.8) mg/kg; KU-32 = 1.2 (0.87 – 1.5) mg/kg; 3.5 fold increase in potency.

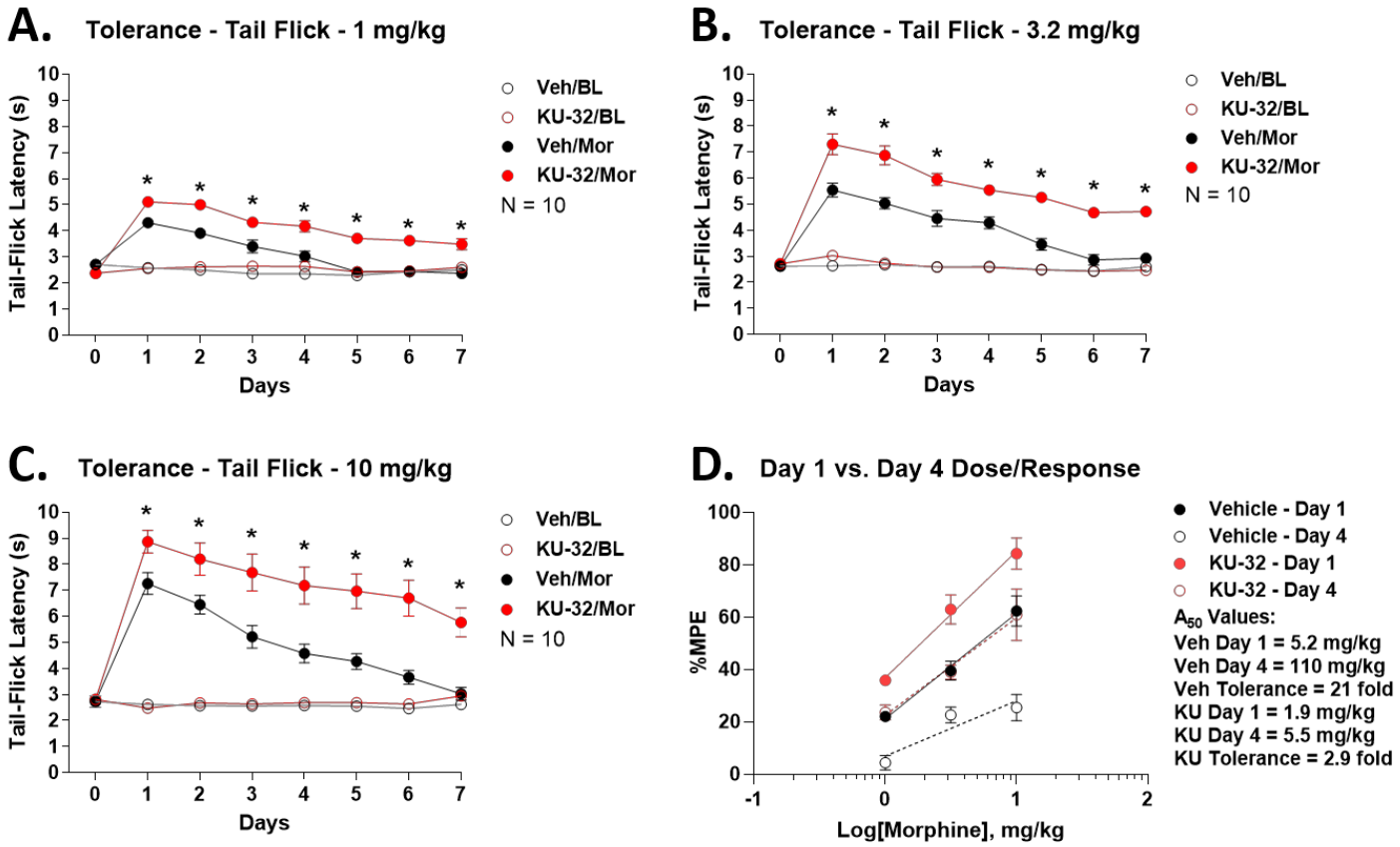

Figure 4: Spinal Hsp90 inhibition reduces morphine anti-nociceptive tolerance. Male and female CD-1 mice injected with 0.01 nmol KU-32 or Vehicle control i.t. beginning on day 0 and continuing daily until day 6. The mice were injected with 1-10 mg/kg morphine s.c. twice daily beginning on day 1 and continuing daily until day 7. Thermal tail flick latencies (52°C, 10 sec cutoff) were recorded before treatment on day 0, daily before morphine injection ("BL"), and 30 minutes after each morning morphine injection on days 1-7. Data reported as the mean ± SEM with sample sizes of mice/group noted in the graphs. * = $p < 0.05$ vs. same time point Veh/Mor group by RM 2 Way ANOVA with Tukey's *post hoc* test. **A-C)** Individual dose/time curves shown as labeled. KU-32 treatment caused consistent elevation over Vehicle treatment over the 7 day period in all doses. Data not normalized. **D)** Day 1 vs. Day 4 dose/response analysis performed. Data normalized to %MPE (baseline vs. 10 sec cutoff). A_{50}: Vehicle Day 1 = 5.2 (3.9 – 7.5) mg/kg, Vehicle Day 4 = 110 (30 – 6300) mg/kg, 21 fold shift; KU-32 Day 1 = 1.9 (1.3 – 2.5) mg/kg, KU-32 Day 4 = 5.5 (3.5 – 12) mg/kg, 2.9 fold shift.

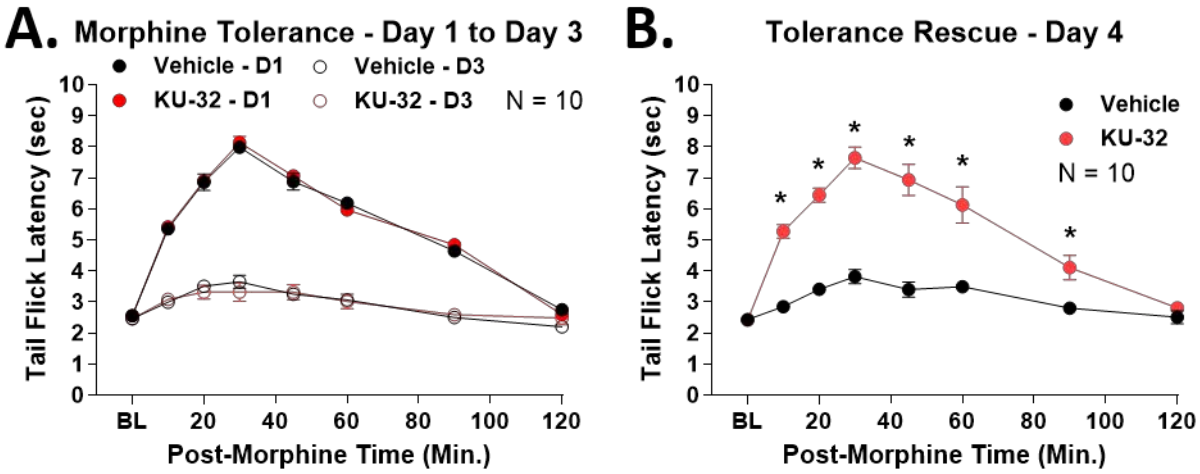

Figure 5: Spinal Hsp90 inhibition rescues established morphine anti-nociceptive tolerance. Male and female mice treated with twice daily morphine (10 mg/kg, s.c.) for 3 days. On day 3, after measuring the tail flick time course, the mice were injected with 0.01 nmol KU-32 or Vehicle control, i.t., with a 24 hour recovery. On day 4, the mice were injected again with 10 mg/kg morphine, s.c.. On days 1, 3, and 4, baseline and post-morphine tail flick latencies (52°C, 10 sec cutoff) were measured. Data reported as the mean ± SEM with the sample size of mice/group noted in the graphs. Experiment performed in 2 technical replicates. * = $p < 0.05$ vs. same time point Vehicle group by RM 2 Way ANOVA with Sidak's *post hoc* test. **A)** Tail flick responses shown on day 1 (acute morphine) and day 3 (morphine-tolerant). No statistically significant differences between the groups at any time point ($p > 0.05$). **B)** Tail flick responses shown on day 4, 24 hours after KU-32 or Vehicle treatment. The KU-32 treated mice, previously tolerant on day 3, showed a statistically significant increase in morphine anti-nociception when compared to Vehicle.

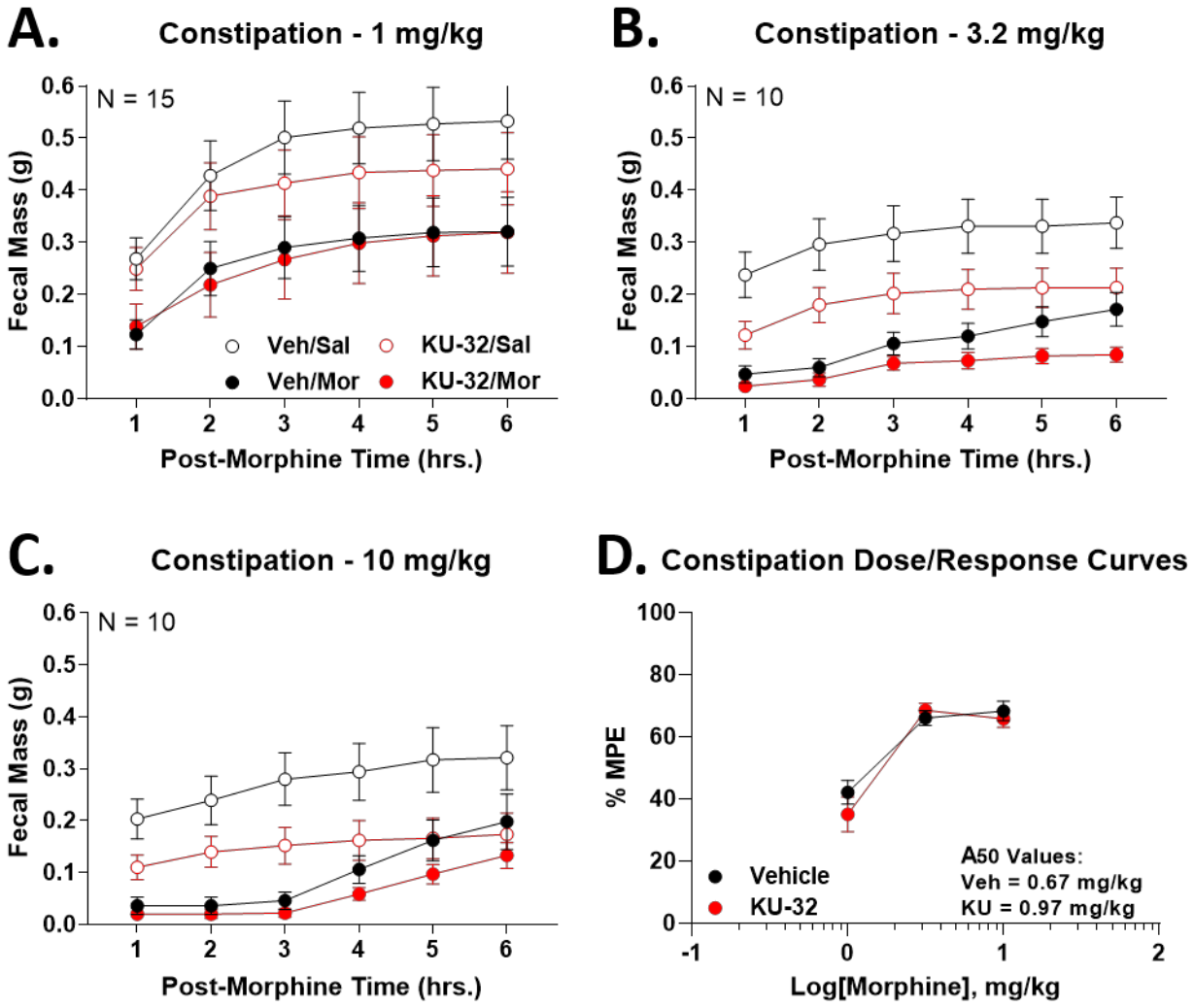

Figure 6: Spinal Hsp90 inhibition does not alter morphine-induced constipation. Male and female CD-1 mice treated with 0.01 nmol KU-32 or Vehicle control i.t., 24 hours, followed by 1-10 mg/kg morphine, s.c.. Fecal mass was measured over 6 hours post-morphine, and used to construct cumulative plots. Curves for morphine as well as saline-injected controls shown. Data reported as the mean ± SEM with the sample size of mice/group noted in the graphs. Experiments performed in 2-3 technical replicates. **A-C)** Individual dose curves reported, along with saline-injected controls. KU-32 treated saline or morphine groups were not statistically different from Vehicle saline or morphine injected groups, respectively, at any time point ($p > 0.05$). **D)** Morphine injected animals were normalized to saline injected controls for each treatment group (Vehicle or KU-32), and used to construct dose/response curves. The 6 hour area under the curve (AUC) data from **A-C** was further normalized to %MPE (100% MPE = 0% fecal production/100% constipation). Only the 1 and 3.2 mg/kg dose curves were used to calculate the A_{50} since the dose response plateaus between 3.2-10 mg/kg. A_{50}: Vehicle = 0.67 (0.32 – 0.94) mg/kg; KU-32 = 0.97 (0.59 – 1.3) mg/kg.

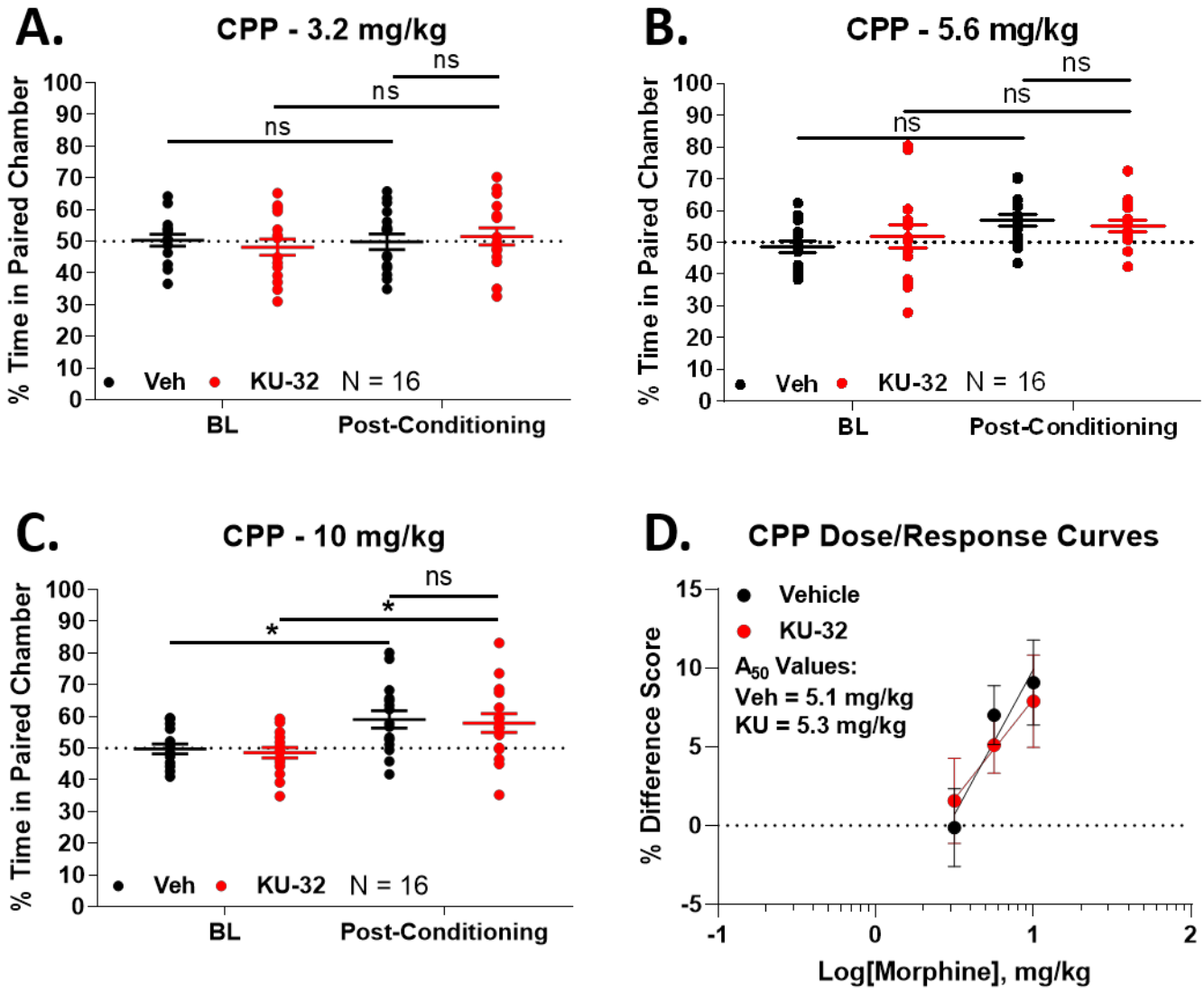

Figure 7: Spinal Hsp90 inhibition does not alter reward learning. Male and female mice were treated over 4 days with KU-32 or Vehicle treatment i.t., combined with 3.2-10 mg/kg morphine, s.c. as a conditioned place preference (CPP) stimulus (see Methods). On day 5, paired chamber preference was recorded. Data reported as the mean ± SEM with the sample size of mice/group noted in the graphs. Each dose performed in 2 technical replicates. * = $p < 0.05$ vs. same treatment Baseline (BL) by RM 2 Way ANOVA with Tukey's *post hoc* test. **A-C)** The individual doses are shown. There was a trend to increasing preference with increasing dose that reached significance over baseline at 10 mg/kg for both Vehicle and KU-32 treatment. There was no difference between Vehicle and KU-32 treatment ($p > 0.05$). **D)** Dose/response analysis was performed, with the data reported as the % Difference Score (see Methods). For the purposes of A_{50} calculation, the response at 10 mg/kg in Vehicle-treated mice was considered to be a maximal response, since 100% preference is not possible in this assay. A_{50}: Vehicle = 5.1 (2.7 – 7.7) mg/kg; KU-32 = 5.3 (-∞ - +∞) mg/kg.